The Pennsylvania State University

The Graduate School

College of Earth and Mineral Sciences

PSEUDO-PRESSURE TYPE CURVE APPROACH

FOR PERMEABILITY AND POROSITY ESTIMATION FROM PRESSURE-PULSE DECAY DATA

A Thesis in

Energy and Mineral Engineering

by

Botros Fouad Baligh Abdelmalek

Submitted in Partial Fulfillment

of the Requirements

for the Degree of

Master of Science

May 2016

The thesis of Botros Fouad Baligh Abdelmalek was reviewed and approved* by the following:

Zuleima T. Karpyn

Associate Professor of Petroleum and Natural Gas Engineering

Thesis Co-Adviser

Shimin Liu

Assistant Professor of Mining Engineering

Thesis Co-Adviser

Luis F. Ayala

Professor of Petroleum and Natural Gas Engineering

Associate Department Head for Graduate Education

*Signatures are on file in the Graduate School.

Abstract

This work presents an improved pseudo-pressure type curve approach to interpret laboratory pulse decay data to estimate rock core permeability and porosity. The proposed method enables the analysis of pulse decay experimental data at low initial pressure and high pulse magnitude. The pseudo-pressure is a mathematical transform that is a function of pressure viscosity and gas deviation factor (Z) that can convert the compressible flow equation from its highly non-linear form to a quasi-linear partial differential equation that can be solved in a simple way without assuming small changes in the viscosity and compressibility. The pseudo-pressure approach resolves calculation problems incurred due to changes in gas viscosity and compressibility during the course of the pulse decay experiment. The type curve analysis proposed in this work allows for comparison of experimental data with theoretical curves generated from analytical models.

Five pulse decay experiments were performed at pore pressures ranging from 130 psi to 700 psi in a tri-axial cell to estimate permeability and porosity of ultra-tight shale cores. The experiments were made in an increasing order of equilibration pressure starting from 130 psi until 700 psi, the pressure-pulse was of a relatively large magnitude that is equal to 200 psi and vertical and radial stresses were kept constant at 1500 psi. Permeability estimates from the proposed pseudo-pressure approach, which is based on the compressible flow equation, was compared with the Jones method that is based on the slightly compressible flow model. This comparison demonstrates that the proposed method is able to detect the changes of permeability as a function of stress conditions in more accurate way. There are two main reasons

for the inability of the Jones method to detect those changes in permeability. First, the changes in the product of viscosity and compressibility were significant during the pulse decay experiments done in this work and the slightly compressible flow equations assume it to be constant. Second, the Jones method equations had some approximations that can work for a certain range of experimental designs in terms of upstream and downstream volumes sizes relative to each other and to the pore volume. However, the proposed method can accommodate the changes in viscosity and compressibility because the pseudo pressure approach is based on the compressible flow equation. In addition, the proposed method does not have any approximations as it deals with the generalized solution; therefore, the range of experimental designs that it can analyze in terms of upstream, downstream and sample volumes is much wider.

Pulse decay experiments at low pressures as demonstrated in this work are useful to describe shale gas reservoirs during its depletion period, and this work demonstrates the pseudo-pressure approach to be suitable for analyzing the pulse decay experiments at low pressures with high pulse magnitude. Consequently, providing a more accurate estimate of sample porosity and permeability for a wide range of system setups.

Table of Contents

List of Tables

List of Figures

Nomenclature

A = cross-sectional area of the core, in^2

c_{gui} = Gas compressibility in the upstream at the value of initial upstream pressure right after applying the pulse

$c_{gdi} =$ Gas compressibility in the downstream at a pressure value of equilibration pore pressure, psi^{-1}

c_{gp}= Gas compressibility at initial pore pressure, psi^{-1}

c_{tp}= Total compressibility at initial pore pressure, psi^{-1}

$f_1 =$ "mass flow correction factor", from (Jones 1997)

$k =$ Permeability, md

L = Length of the core, in

m_1= The slope of dimensionless pressure vs time data, sec^{-1}

P = Pressure, psia

$P_d =$ downstream pressure, psi

$(P_{eq})_p$ = equilibration pseudo pressure, $psia^2/cp$

P_o = initial Pore pressure, psia

P_p = Pseudo Pressure, $psia^2/cp$

P_{pd} = Downstream Pseudo Pressure, $psia^2/cp$

P_{pp} = Pulse Pseudo Pressure, $psia^2/cp$

P_{pu} = Upstream Pseudo Pressure, $psia^2/cp$

P_u = Upstream pressure, psi

V_u = Upstream volume, in^3

V_d = Downstream volume, in^3

z = Compressibility factor, dimensionless

α = dimensionless time

β = ratio of compressive storage in the sample to the compressive storage in the downstream volume, dimensionless

γ = ratio of compressive storage in the downstream to the compressive storage in the upstream, dimensionless

θ_m = roots of the equation

μ = viscosity, cp

μ_{ui} = viscosity of the fluid in the upstream at time=0, cp

μ_{di} = viscosity of the fluid in the downstream at time=0, cp

μ_p = viscosity at initial pore pressure, cp

ϕ = porosity, fraction

Chapter 1. Introduction

It has been shown in a study that many of the gas reservoirs in the US have started production at an initial pressure between 400 psi to 4000 psi (Shi et al. 2013). At such pressure range, the changes in gas properties, in addition to the changes in stress conditions, can affect the permeability of Shale gas reservoirs; and thus, their productivity. Obtaining rock permeability through lab measurements, if properly up-scaled, can serve as a good estimate for reservoir permeability. Moreover, it is important to be able to do those permeability measurements on rocks at conditions of pressure and temperature that are similar to where they were originally extracted from. However, not all of the well-established methods for lab-scale permeability measurements for tight rocks can accurately obtain the permeability at low pressure in particular. Not only that, the methods that can calculate permeability at low pressures for tight rocks have problems related to the time needed to finish the experiment. For example: Permeability measurement for tight rocks using a steady state method is demanding in terms of time (Zamirian et al. 2014), as a steady flow can easily take weeks to be established in such rocks like shale and coal. Since the steady state methods are slow to estimate permeability, other methods have been introduced to measure the permeability of tight rocks. Some of the relatively recent methods are pulse decay (Brace, Walsh, and Frangos 1968; Hsieh et al. 1981; Dicker and Smits 1988; Jones 1997),crushed sample technique (Cui, Bustin, and Bustin 2009), pore pressure oscillations (Fischer 1992) and complex pore pressure transients (Boitnott 1997).

Each of the aforementioned recent methods has its advantage and disadvantage. Crushed sample method is the simplest method where only two chambers of known volumes are needed

and gas is allowed to expand into the crushed sample chamber from a reference chamber (Cui, Bustin, and Bustin 2009; Zamirian et al. 2014). Using pressure and time data, one can calculate the permeability. One of the disadvantages of this method is that getting permeability response as a function of stress conditions is not possible, as stress cannot be applied on such sample. The pulse decay technique requires sending a pressure pulse from the upstream volume, which will permeate through the sample to a downstream volume (Brace, Walsh, and Frangos 1968; Hsieh et al. 1981; Dicker and Smits 1988; Jones 1997). The Pressure decay response is continuously recorded with time and then sample permeability is estimated by interpretation of pressure decay curve. The benefit from the pulse decay is the time reduction in obtaining permeability of tight samples. However, as will be discussed thoroughly in this work, the current models do not accurately deal with pulse decay experiments at low pressures. Pore pressure oscillations method was proposed in order to tackle the problem of getting noisy signal from the pulse decay technique. In this method, sinusoidal pore pressure pulse is sent from the upstream of the sample and based on the retardation of the signal and phase change at the downstream, permeability can be calculated (Fischer 1992; Jin et al. 2015). However, recent pressure transducers do not cause noisy signals that requires a new modification on enhancing the signal, especially when the signal is clear from a simpler measurement technique like the pulse decay. Finally, complex pore pressure oscillations method is similar to the pore pressure oscillations methods, but instead of sending a sinusoidal pore pressure pulse from the upstream, different pore-pressure pulses that are more distinct are sent; for example: MULTSINE which is a pulse that is made by three sinusoidal waves (Boitnott 1997). This method has an advantage over the pore pressure oscillations that it can do measurements for high permeability samples; however, it still adds

complexity that is unneeded as the same measurements can be done in a simpler manner. Therefore, it was found in this work, that the pulse decay is a method that offers a good degree of accuracy and speed with the minimum amount of work needed.

The data from the pulse decay experiment can be manipulated in two different ways: a straight-line method (Brace, Walsh, and Frangos 1968; Dicker and Smits 1988; Jones 1997) and type curve matching (Hsieh et al. 1981; Neuzil et al. 1981; Haskett, Narahara, and Holditch 1988; Kamath, Boyer, and Nakagawa 1992). “Straight-line” method requires to determine the slope of the straight line in the semi-log plot of pressure decay versus time. Based the estimated slope, the permeability can be estimated since it is the only unknown parameter in the analysis. On the other hand, Type Curve matching is to compare theoretical curves that are generated from fluid flow mathematical models in terms of dimensionless parameters. Once the match points between theoretical and experimental data are identified, both permeability and porosity can be determined. Regardless of the types of manipulation, one has to choose the most appropriate mathematical model or governing equation that can represent the fluid flow during the experiment, e.g. incompressible, slightly compressible or compressible flow.

The pulse decay approaches can be categorized based on the governing equations and methods of data interpretation. First, (Brace, Walsh, and Frangos 1968) used the incompressible flow equation as a governing equation and the straight-line method as a data manipulation method. However, the incompressible flow model cannot capture the physics of compressible fluids, (Brace, Walsh, and Frangos 1968) method can give correct permeability trends instead of correct permeability values, for example, detecting changes of permeability as function of stress conditions, water content and heterogeneity. Second, (Hsieh et al. 1981; Neuzil et al. 1981) used

the slightly compressible flow equation as the governing equation and type curve matching as a method of data manipulation. It should be mentioned that (Hsieh et al. 1981) work presented the generalized solutions and used the type curve approach to assess the whole experimental data rather than a section of it whether the early time (Bourbie and Walls 1982) or late time (Dicker and Smits 1988; Jones 1997). The only limitation with their work is that the slightly compressible flow equation is unable to analyze low pressure and high pulse magnitude pressure-decay experiments. Third, (Dicker and Smits 1988) and (Jones 1997) methods do represent the straight-line methods with the slightly compressible equation. Both approaches require designing an identical upstream and downstream volume that needs to be very close to the pore volume. Additionally, those two methods have problems to represent the compressible flow behavior. Finally, (Haskett, Narahara, and Holditch 1988) were the first to propose the use of the pseudo-pressure approach to analyze the pulse decay experiments. The advantage of the pseudo-pressure approach is that changes in viscosity and compressibility during the experiment can be accounted for in the governing equation. However, (Haskett, Narahara, and Holditch 1988) method had three limitations. First, the method requires the conversion of the differential pressure data to pseudo-pressures, which can be problematic due to the non-linear relationship between pressure and pseudo-pressure at low pressures. Second, the method demands the use of a pseudo time rather than the real time. This pseudo time was first introduced to fix the problem of well test data that is distorted with wellbore storage effects. Such problem is not encountered in the pulse decay experiments; therefore, there is no need for it. Third, the method requires developing a computer code in order to do the type curve matching automatically. However, there is a method in the literature of Hydrology (Hsieh et al. 1981; Neuzil et al. 1981)

that did the type curve matching in a simpler way, where only one type curve that is specific to the experimental setup was generated and estimates for the porosity and permeability for a wide range were made. Therefore, a considerable amount of work could be saved while achieving the same results.

Among the methods described, the pseudo pressure approach would be the most accurate way for analyzing the pulse decay experiments with gases because the pseudo pressure approach is based on the compressible flow equation; therefore, the method can accurately describe the behavior of gases especially at low pressures. The only method that attempted to apply the pseudo pressure approach (Haskett, Narahara, and Holditch 1988) has some limitations. Those limitations, as mentioned previously, had to do with converting the difference in pressure between the upstream and downstream to pseudo pressures, the use of the pseudo time that is not needed in the pulse decay experiment and the unnecessary amount of work for the type curve matching. Therefore, there is a need to accurately and efficiently treat compressible fluids pulse decay experiments and estimate the permeability and porosity using the pseudo pressure approach with type curve matching.

In this work, a pseudo-pressure type-curve approach is newly proposed to estimate permeability and porosity from gas pulse decay experiments. The newly proposed approach will solve the three limitations that were found in (Haskett, Narahara, and Holditch 1988) work by making three modifications. First, the upstream and downstream pressures are going to be transformed into pseudo pressures, instead of converting the difference in pressure; and thus, the non-linearity between the pressure and pseudo pressures at low pressures are going to be taken in to consideration. Second, this method will not use the pseudo time concept in its

governing equation, as there is no need for it. Third, the type curve approach from the (Hsieh et al. 1981; Neuzil et al. 1981) is going to be used for its simplicity and the amount of work it can be save without affecting its accuracy.

Chapter 2. Model development and procedure to estimate core permeability and porosity

In this work, type curves are generated from the solutions for the compressible flow equation as shown in equation (1). This compressible flow equation is the quasi-linear, partial differential equation developed by (Al-Hussainy, Ramey, and Crawford 1966):

$$\frac{\partial^2 P_p}{\partial x^2} = \frac{\mu_p \phi c_{tp}}{k} \frac{\partial P_p}{\partial t} \tag{1}$$

where, P_p is the pseudo-pressure, μ_p in gas viscosity at initial pore pressure, c_{tp} is total compressibility at initial pore pressure, t is time and k is permeability. In equation (1), the partial differential equation considering the real compressible gas was linearized without the assumptions of constant viscosity and compressibility. This linearization process was implemented by adopting the pseudo-pressure transformation without the small pressure gradient assumption, and it is mathematically given in equation (2).

$$P_p = 2 \int_{P_o}^{P} \frac{P}{\mu z} dp \tag{2}$$

Equation (1) was developed by doing a one-dimensional mass balance as following:

$$mass\ in - mass\ out = Storage$$

Figure (1): 1D mass balance shown on a small sample similar to the one used in this work

$$\dot{m}_{in}\Delta t - \dot{m}_{out}\Delta t = \left(V_b \phi \rho_g\right)_{t+\Delta t} - \left(V_b \phi \rho_g\right)_t \tag{3}$$

$$\dot{m} = \rho_g v_g A \tag{4}$$

$$\left(\rho_g v_g A\right)_{in} - \left(\rho_g v_g A\right)_{out} = \frac{V_b \phi}{\Delta t} . \left(\Delta \rho_g\right) \tag{5}$$

If both sides of the equation are divided by V_b, we get:

$$\left(\frac{\rho_g v_g}{\Delta x}\right)_{in} - \left(\frac{\rho_g v_g}{\Delta x}\right)_{out} = \frac{\phi}{\Delta t} . \Delta \rho_g \tag{6}$$

If we take the limit of equation (6) when $\Delta x \to 0$ and $\Delta t \to 0$, we get equation (7):

$$-\frac{\partial}{\partial x}\left(\rho_g v_g\right) = \frac{\partial}{\partial t}\left(\phi \rho_g\right) \tag{7}$$

The model in this work assumes that advection or Darcian flow is the only dominant flow regime; therefore, the velocity of gas term, v_g, is going to be replaced by Darcy's law as following:

$$v_g = -\frac{k}{\mu} . \frac{dP}{dx} \tag{8}$$

If Darcy's law is added to the continuity equation, the following equation will be the result:

$$-\frac{\partial}{\partial x}\left(\rho_g \left(-\frac{k}{\mu} . \frac{dP}{dx}\right)\right) = \frac{\partial}{\partial t}\left(\phi \rho_g\right) \tag{9}$$

The model assumes that k and ϕ are constants because the sample is small. However, the model assumes that the fluid used is a compressible one.

$$\rho_g = \frac{P.MW}{Z.R.T} \tag{10}$$

$$k.\frac{\partial}{\partial x}\left(\frac{1}{\mu}.\frac{P.MW}{Z.R.T}\left(\frac{dP}{dx}\right)\right) = \phi.\frac{\partial}{\partial t}\left(\frac{P.MW}{Z.R.T}\right) \tag{11}$$

MW, R and T are going to be cancelled from both sides, then we get:

$$k.\frac{\partial}{\partial x}\left(\frac{P}{\mu.Z}\left(\frac{dP}{dx}\right)\right) = \phi.\frac{\partial}{\partial t}\left(\frac{P}{Z}\right) \tag{12}$$

As can be seen in equation (12), it is a highly non-linear equation due to the presence of terms like the μ and Z that depends on the pressure. Therefore, the pseudo pressure transform (Al-Hussainy, Ramey, and Crawford 1966) that is in equation (2) is going to be added to simplify the equation:

If we take the derivative for both sides for equation (2), we get equation (13):

$$dP_p = \frac{P}{\mu Z}dP \tag{13}$$

$$dP = \frac{\mu Z}{P}dP_p \tag{14}$$

By adding equation (14) to the left hand side (LHS) of equation (12), the LHS becomes:

$$LHS = \ k.\frac{\partial}{\partial x}\left(\frac{P}{\mu.Z}.\frac{\mu Z}{P}\left(\frac{dP_p}{dx}\right)\right) = k.\frac{\partial^2 P_p}{\partial x^2} \tag{15}$$

If we did the some mathematical manipulation to the right hand side (RHS) of equation (12) we get equation (21). This mathematical manipulation is shown in equations 16 to 20.

$$\frac{\partial}{\partial t}\left(\frac{P}{Z}\right) = \frac{\partial}{\partial P}\left(\frac{P}{Z}\right)\frac{\partial P}{\partial t} \tag{16}$$

$$\frac{\partial}{\partial t}\left(\frac{P}{Z}\right) = \left[\frac{\left((1)(Z) - \frac{\partial Z}{\partial P}.P\right)}{Z^2}\right].\frac{\partial P}{\partial t} \tag{17}$$

$$\frac{\partial}{\partial t}\left(\frac{P}{Z}\right) = \left[\frac{1}{Z} - \frac{P}{Z^2}.\frac{\partial Z}{\partial P}\right]\frac{\partial P}{\partial t} \tag{18}$$

$$\frac{\partial}{\partial t}\left(\frac{P}{Z}\right) = \frac{P}{Z}\left[\frac{1}{P} - \frac{1}{Z}.\frac{\partial Z}{\partial P}\right]\frac{\partial P}{\partial t} \tag{19}$$

$$c_g = \frac{1}{P} - \frac{1}{Z}.\frac{\partial Z}{\partial P} \tag{20}$$

$$\frac{\partial}{\partial t}\left(\frac{P}{Z}\right) = \frac{Pc_g}{Z}\frac{\partial P}{\partial t} \tag{21}$$

By adding equations (15) and (21) in equation (12), we would get equation (22)

$$k.\frac{\partial^2 P_p}{\partial x^2} = \phi\frac{Pc_g}{Z}\frac{\partial P}{\partial t} \tag{22}$$

Finally, if we replaced the ∂P with its definition in terms of pseudo pressure as shown in equation (23), we get the governing partial differential equation (24).

$$k.\frac{\partial^2 P_p}{\partial x^2} = \phi\frac{Pc_g}{Z}.\frac{\mu Z}{P}.\frac{\partial P_p}{\partial t} \tag{23}$$

$$\frac{\partial^2 P_p}{\partial x^2} = \frac{\phi.\mu.c_g}{k}\frac{\partial P_p}{\partial t} \tag{24}$$

In order to solve the governing equation for the pressure pulse-decay experiments, the boundary conditions need to be specified and they are as follows:

$$P_p(x,0) = \left(P_{eq}\right)_p \text{ for } 0 < x < L \tag{25}$$

$$P_p(0,t) = P_{pd}(t) \text{ for } t > 0 \tag{26}$$

$$P_p(L,t) = P_{pu}(t) \text{ for } t > 0 \tag{27}$$

$$\frac{\mu_{ui} c_{gui} V_u}{kA} \frac{\partial P_{pu}}{\partial t} - \left(\frac{\partial P_p}{\partial x}\right)_{x=L} = 0 \text{ for } t > 0 \tag{28}$$

$$P_{Pu}(0) = P_{pp} \text{ for t=0} \tag{29}$$

$$\frac{\mu_{di} c_{gdi} V_d}{kA} \frac{\partial P_{pd}}{\partial t} - \left(\frac{\partial P_p}{\partial x}\right)_{x=0} = 0 \text{ for } t > 0 \tag{30}$$

$$P_{Pd}(0) = 0 \text{ for t=0} \tag{31}$$

Equation (25) states that the pseudo pressure throughout the sample at time = 0, $P_p(x,0)$, is equal to the equilibrated pseudo pressure $\left(P_{eq}\right)_p$. Equation (26) describes that the pseudo pressure at the end of the sample that is in contact with the downstream reservoir $P_p(0,t)$ has the same value as the pseudo pressure in the downstream reservoir $P_{pd}(t)$ at any time during the experiment. Similar to equation (26), equation (27) illustrates that the pseudo pressure at the other end of the sample $P_p(L,t)$ has a pseudo pressure value that is same to the one in the upstream reservoir $P_{pu}(t)$ during the experiment. Equation (28) is a result of a mass balance done at the upstream end of the sample, where μ_{ui} is the viscosity of the fluid used in the experiment in upstream reservoir at time=0, c_{gui} is the fluid compressibility in the upstream reservoir at time=0, V_u is the upstream volume, and A is the cross-sectional area of the sample that is perpendicular to the flow. Equation (30) is similar to equation (28); however, the mass balance

is done on the downstream end of the sample, where μ_{di} is the viscosity of the fluid used in the experiment in downstream at time=0, c_{gdi} is the fluid compressibility in the downstream reservoir at time=0, V_d is the downstream volume. Equation (29) states that the upstream pseudo pressure at time=0, $P_{pu}(0)$, is equal to the pseudo pulse pressure P_{pp}. Equation (31) is similar to equation (29), but for the downstream side. Based on the boundary conditions taken in equations (29) and (31), the type curves produced from this mathematical model will be bounded between 0 and 1.

The governing equation (1) with its boundary conditions (25-31) can be solved by the Laplace transform method. The solutions for dimensionless pseudo pressures for upstream and downstream are given in equations (32) and (33); those two equations were first developed by (Hsieh et al. 1981) and then (Haskett, Narahara, and Holditch 1988) adapted them to be used for the pseudo pressure approach.

$$\frac{P_{pu}}{P_{pp}} = \frac{1}{1+\beta+\gamma} + 2\sum_{m=1}^{\infty}\left[\left(\frac{\left(\beta+\frac{\gamma^2\phi_m^2}{\beta}\right)}{\frac{\gamma^2\phi_m^4}{\beta^2}+\frac{(\gamma^2\beta+\gamma^2+\gamma+\beta)\phi_m^2}{\beta}+(\beta^2+\gamma\beta+\beta)}\right)e^{-\alpha\phi_m^2}\right] \tag{32}$$

$$\frac{P_{pd}}{P_{pp}} = \frac{1}{1+\beta+\gamma} + 2\sum_{m=1}^{\infty}\left[\left(\frac{\left(\beta-\frac{\gamma\phi_m^2}{\beta}\right)}{\left[\frac{\gamma^2\phi_m^4}{\beta^2}+\frac{(\gamma^2\beta+\gamma^2+\gamma+\beta)\phi_m^2}{\beta}+(\beta^2+\gamma\beta+\beta)\right]cos\phi_m}\right)e^{-\alpha\phi_m^2}\right] \tag{33}$$

In the above generalized solutions, there are three dimensionless variables α, β, and γ. The first one is (α) and is known as the dimensionless time. Second one is (γ) which is defined as the ratio of the compressive storage of the downstream to compressive storage of the upstream. Third one is (β) which is defined as the ratio of the compressive storage of sample to

the compressive storage of upstream. They are mathematically given in equations (34), (35) and (36):

$$\alpha = \frac{kt}{94812L^2\mu_p\phi C_{tp}} \tag{34}$$

$$\gamma = \frac{V_d}{V_u} \tag{35}$$

$$\beta = \frac{V_p c_{tp}}{V_u c_{gui}} \tag{36}$$

The terms "compressive storage" of upstream, downstream or sample that appeared in last paragraph are defined as the change of the volume of a fluid per unit change in pressure for the upstream, downstream or sample respectively.

Additionally, another parameter in the general solution is ϕ_m which is defined as the roots of the following equation:

$$tan\phi_m = \frac{(1+\gamma)\phi_m}{\frac{\gamma\phi_m^2}{\beta} - \beta} \tag{37}$$

Figure (2) is an example of the pseudo pressure type curves obtained when $\gamma = 1$. The γ (equation 35) is experimentally obtained from the measured upstream and downstream volumes in the experimental assembly. The type curves are computed at a constant γ as the volumes of the upstream and downstream are unchanged during the course of experiments. The β values vary between 0.001 and 10, because the type curves will overlap for β values below 0.001 and above 10 (Hsieh et al. 1981). The ϕ_m (equation 37) is computed, in this work, numerically as shown in detail in appendix A. Finally, the dimensionless time (α) is increasingly changed until

upstream and downstream pressures meet at $\frac{P_{pu}}{P_{pp}} = \frac{P_{pd}}{P_{pp}} = \frac{1}{1+\beta+\gamma}$. The family of type curves in figure (2) also match those constructed by (Hsieh et al. 1981), which is used here as a validation of the proposed method.

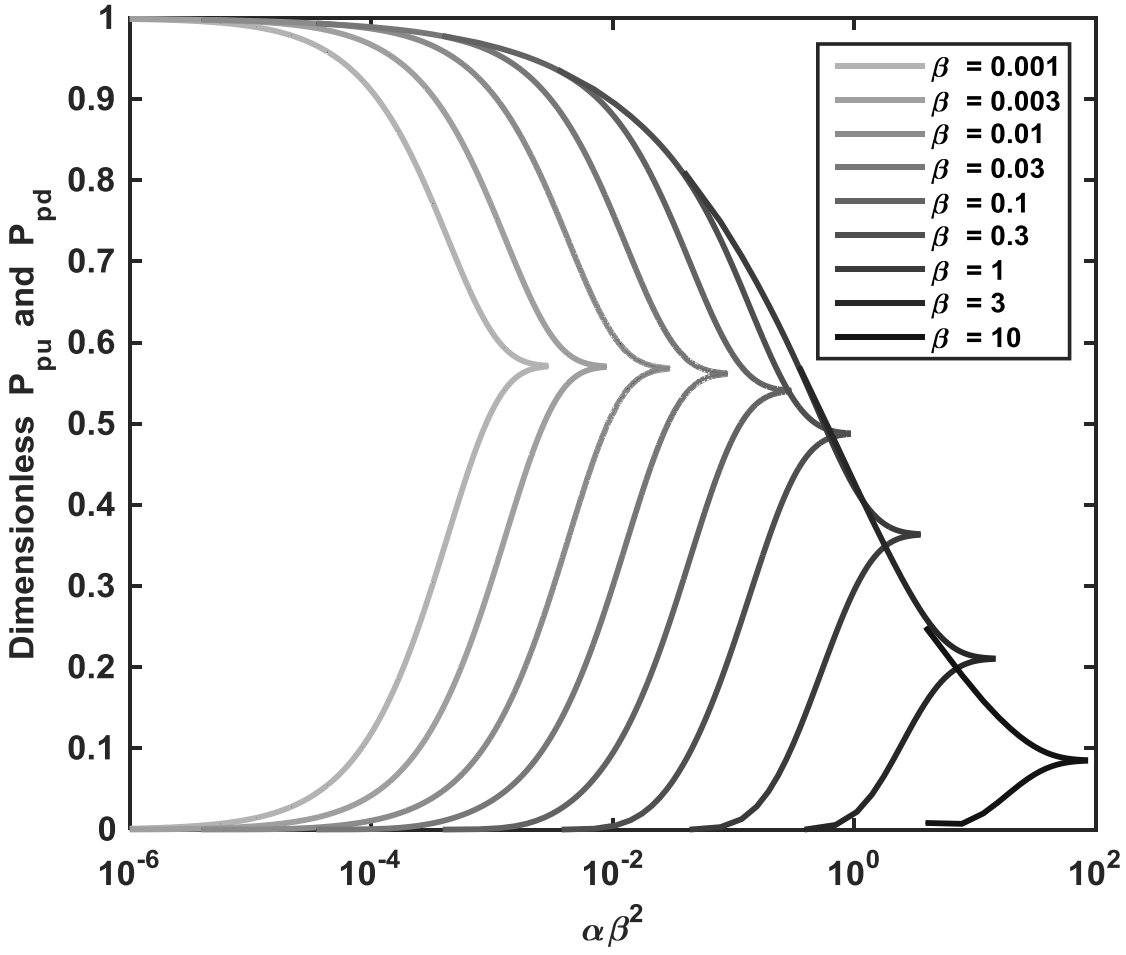

Figure 2: Familly of type curves for $\gamma = 1$ and β between 0.001 and 10 constructed using pseudo-pressure type curves

In order to estimate rock core porosity and permeability from pulse decay experimental data, one can generate a family of system specific type curves, such as those presented in Figure 1, and identify the matching curve for the actual laboratory data of decay pseudo-pressures. The experimental upstream and downstream decay pressures must be converted to the pseudo-pressure domain as described in Appendix B, and normalized using the following two equations:

$$P_{pu}(t)_{normalized} = \frac{P_{pu}(t) - P_{pd}(0)}{P_{pu}(0) - P_{pd}(0)} \tag{38}$$

$$P_{pd}(t)_{normalized} = \frac{P_{pd}(t) - P_{pd}(0)}{P_{pu}(0) - P_{pd}(0)} \tag{39}$$

Finally, the family of type curves and the transformed experimental data are superposed on the same graph to find a fitting match. A match point on the selected match curve is then used to determine $\beta, \alpha\beta^2, and\ time$, which are then used to calculate porosity and permeability with equations (40) and (41).

From β, one can calculate the porosity using equation (40):

$$\phi = \beta \left[\frac{V_u}{AL}\right]\left[\frac{c_{gui}}{c_{tp}}\right] \tag{40}$$

From β and α, one can calculate permeability using equation (41):

$$k = \left[\frac{94812\mu_p c_{tp} V_u^2}{tA\phi}\right].\left[\frac{c_{gui}}{c_{tp}}\right]^2 .[\alpha\beta^2] \tag{41}$$

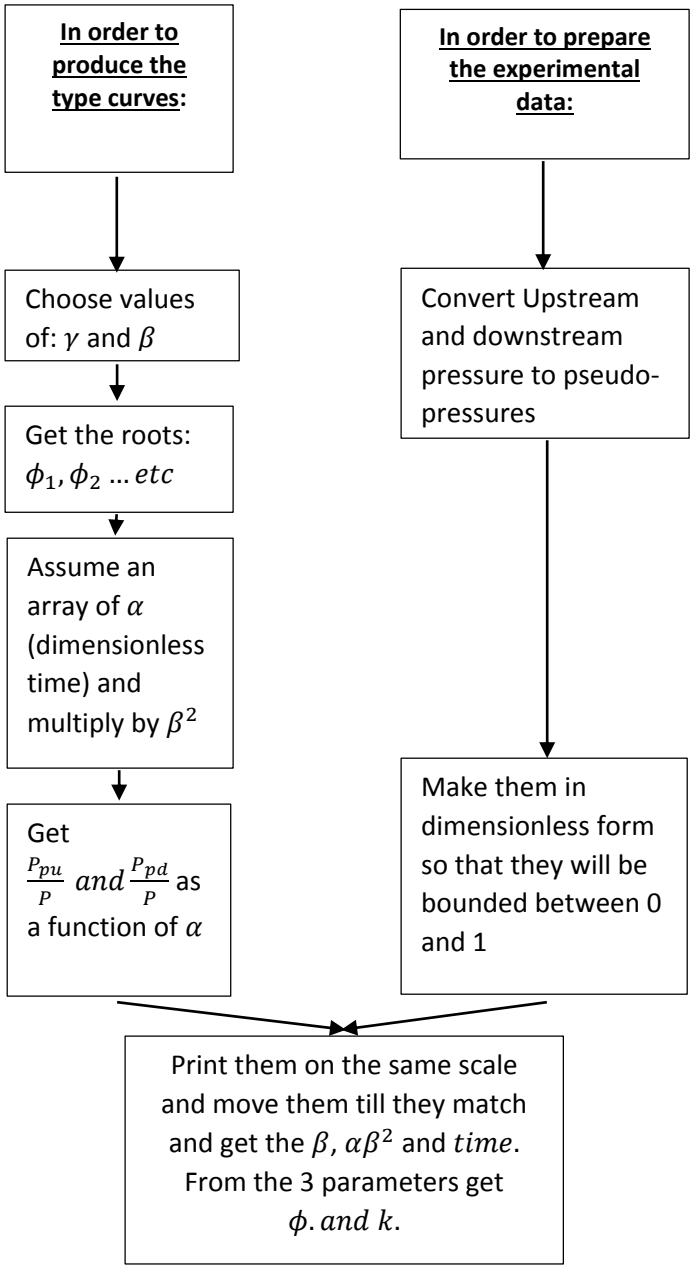

Figure 3: A Flow chart to summarize the main three steps in the process of obtaining permeability and porosity using the type curve-pseudo pressure approach

Chapter 3. Model implementation using experimental data

A laboratory experiment with five pulse decay sequences was conducted on a Marcellus shale core at pore pressures ranging from 130 psi to 700 psi. In the five sequences, both the vertical and radial stresses were kept constant at 1500 psi. Figure 4 shows the experimental assembly used for these sequences. It consists of a triaxial cell, Quizix pump, two omega pressure sensors, a data acquisition system (DAQ) and a high pressure argon cylinder. Sample dimensions were 2.54 cm diameter and 5.715 cm length.

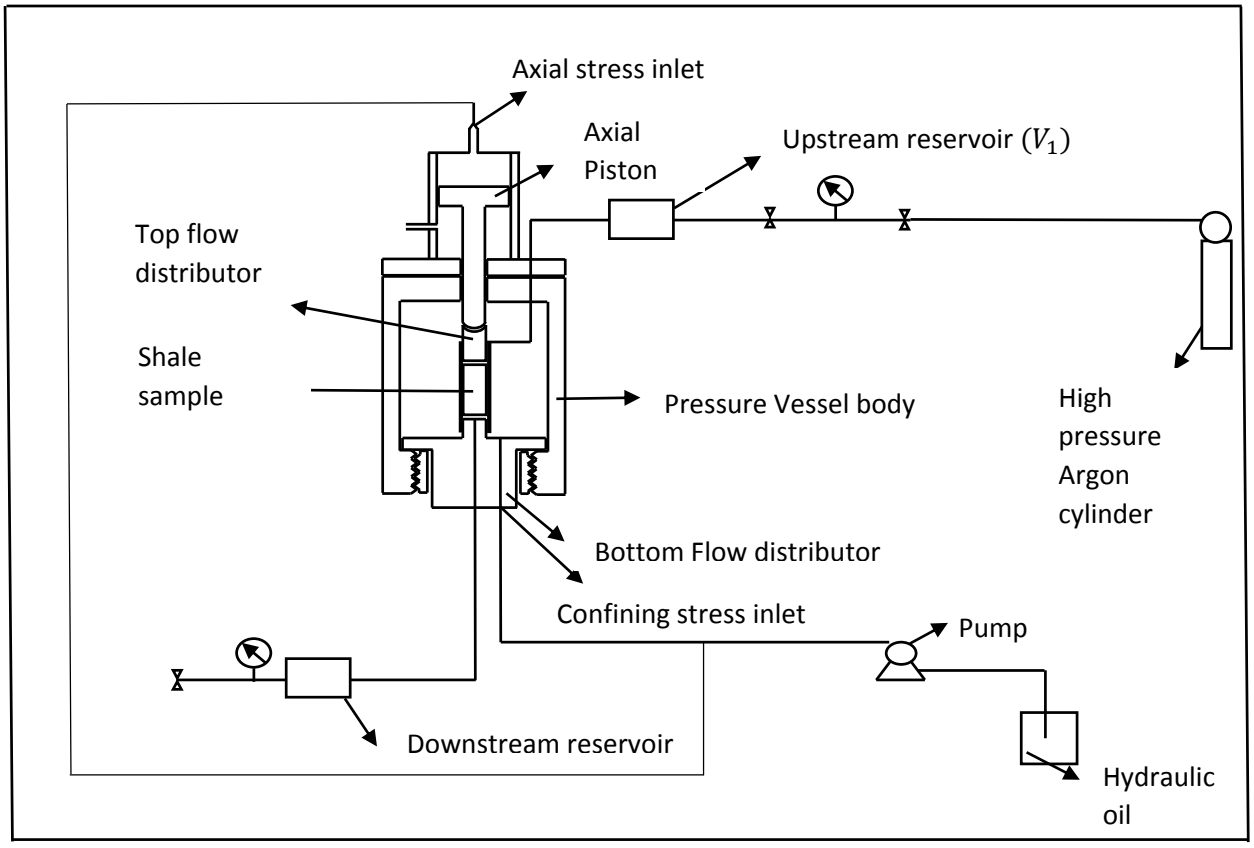

Figure 4: Schematic diagram of tri-axial cell and experimental assembly

The experiment starts by setting both vertical and radial stresses on the sample to 1500 psi using one Quizix pump by branching out the pump outlet to feed both the confining stress and axial load inlets as shown in figure (4). Then, the pore pressure was equilibrated to 130.5 psi including the upstream and downstream volumes. Later, a pressure pulse of an approximate magnitude of 200 psi was introduced from the upstream side of the system. The pressure response in both upstream and downstream volumes is recorded at a sampling rate of 1 pressure reading per 600 milliseconds until upstream and downstream pressures equilibrate. In the same manner, four additional pulse decays were performed at increasingly higher upstream pressures, using similar pulse magnitudes of 200 psi. Figure 5 shows five pulse decay sequences and the corresponding pressure profiles.

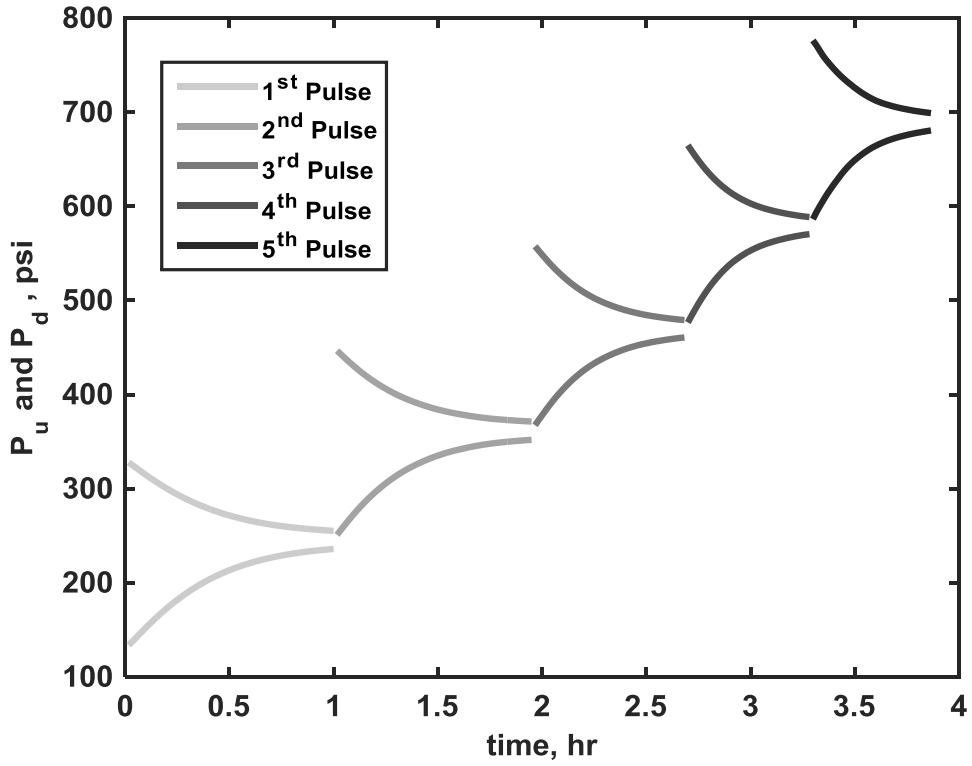

Figure 5: Pressure history of pulse decay experiment in Marcellus shale core

Chapter 4. Results

In this section, four major pieces of results are going to be presented. First, the effect of the pseudo pressure transformation on the pulse decay data. Second, a detailed calculation for permeability and porosity for one of the pulse decay sequences in this work using the proposed method is going to be shown. Third, the results for the permeability in the five sequences using the proposed method. Fourth, the permeability results for the five sequences using the Jones method.

Figures 6 a, b, and c show the effect of the pseudo pressure transformation on the pressure data. As can be seen, figure 6a shows the normalized real pressure pulse decay data for the 1^{st} pulse decay sequence and on the same plot, the normalized pseudo pressure pulse decay data for the same sequence is shown. Additionally, figure 6b shows the same thing in figure 6a; however, it is done on the 5^{th} sequence. Figure 6c shows 5 points; every point is the difference between the final normalized real pressure and the final normalized pseudo pressure for all five sequences. It is worthwhile to note that from the 1^{st} sequence to the 5^{th} sequence, this difference between the normalized final real pressure and the normalized final pseudo pressure was decreasing. In other words, the higher the final equilibration pore pressure, the more the pseudo pressure transformation becomes of almost no effect as both curves would be the same.

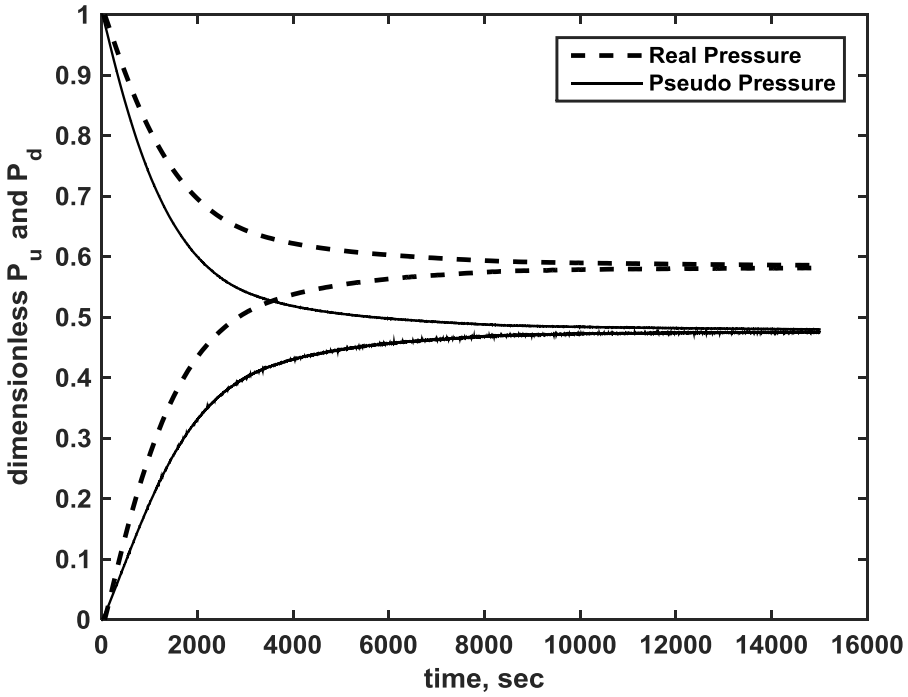

Figure 6a: normalized real and pseudo pressure data for the 1st sequence

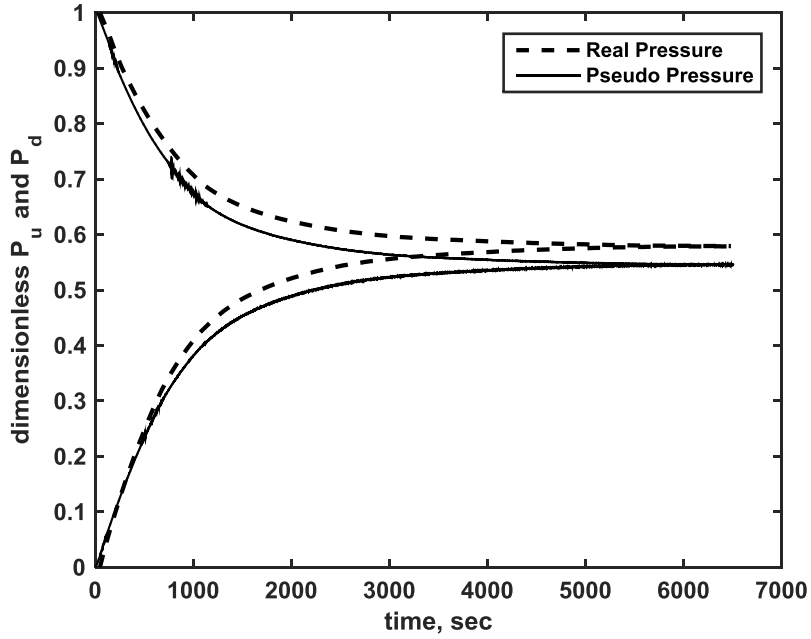

Figure 6b: normalized real and pseudo pressure data for the 5th sequence

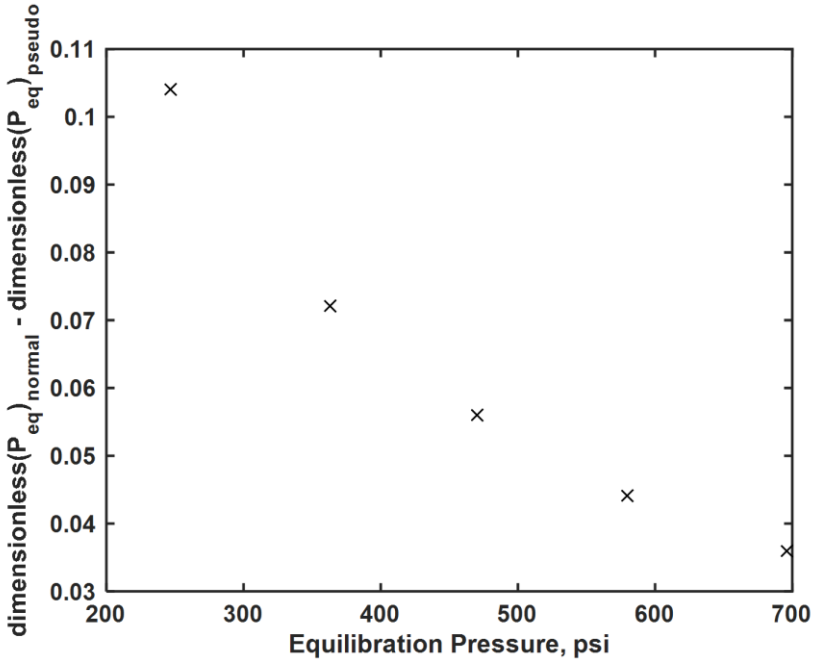

Figure 6c: The difference between the final normalized real pressure and normalized pseudo pressure for the five pulse decay sequences

Figure 6: Effect of the pseudo pressure transformation on the shape of the normalized experimental data

Secondly, a detailed calculation for permeability and porosity for the 5th sequence using the proposed method is going to be presented. This sequence was run at an initial pore pressure of 580 psig, pulse of 200 psig and a final pressure of 696.5 psig. The three steps that were discussed in the "Model Development" section are going to be shown being implemented.

After measuring the upstream and downstream volumes of the experimental setup, the $\gamma = \frac{V_d}{V_u}$ was found to be equal to 0.75. Based on that, the following type curves (figure 7) were generated using the generalized solution for values of β between 0.001 and 1.

Figure 8 shows the pulse decay profile for the 5th pulse being normalized between zero and one for both real pressures and pseudo pressures.

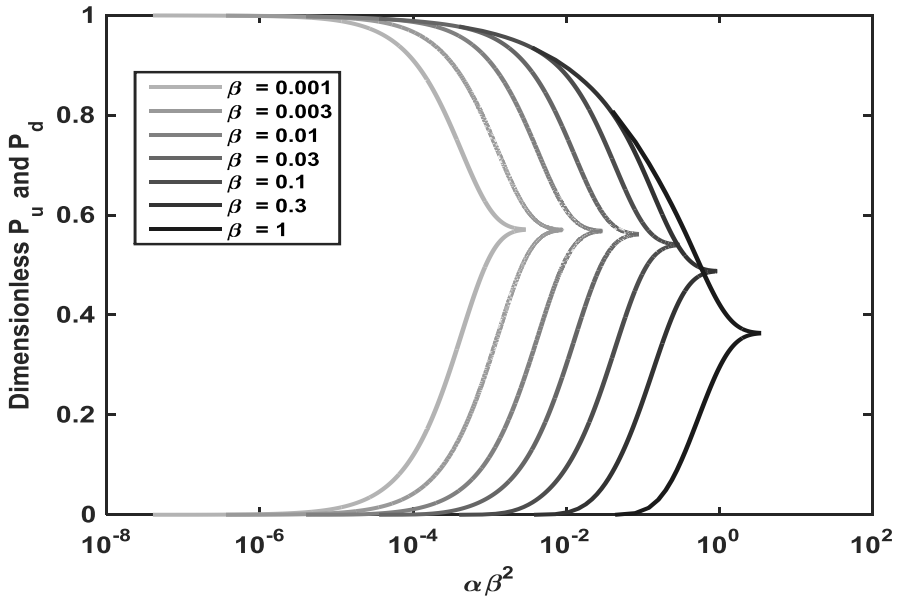

Figure 7: Family of type curves specific to experimental setup

Finally, figure 9 shows, on the left, the type curves and experimental transformed data printed on the same plot. On the same figure, on the right, it can be shown the curves being translated until the best fit is found. Since every curve represents a different value of β, the β is found for this experiment to be 0.09. After that a match point between the two x-axes is found and from this match $\alpha\beta^2$ and time can be obtained. The early time mismatch that is noticed in the upstream is going to be discussed in details in the discussion.

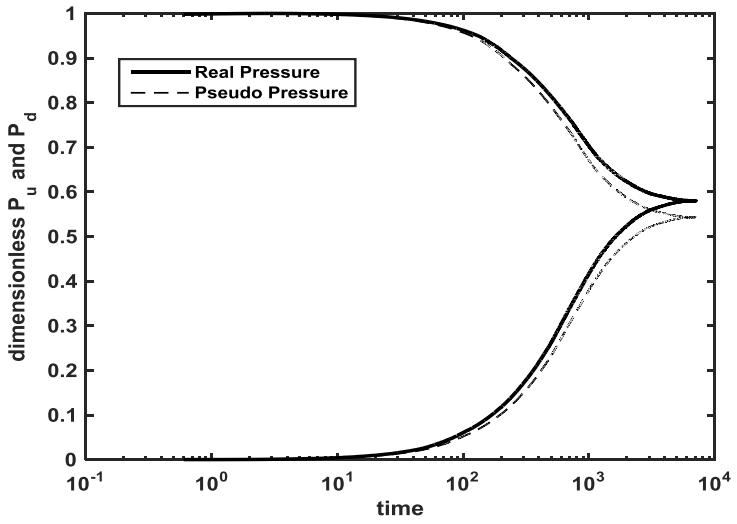

Figure 8: A selected sequence showing the real pressure and pseudo-pressure after normalization

After doing the type curve matching, as shown in figure 9, the following parameters are obtained:

- $\beta = 0.09$
- $\alpha\beta^2 \; at \; match \; point = 0.044$
- Time at match point= 1070 sec

From these data, both permeability and porosity can be calculated using equations (40) and (41):

$$k = 72 \; \mu D$$

$$\phi = \; 3 \; \%$$

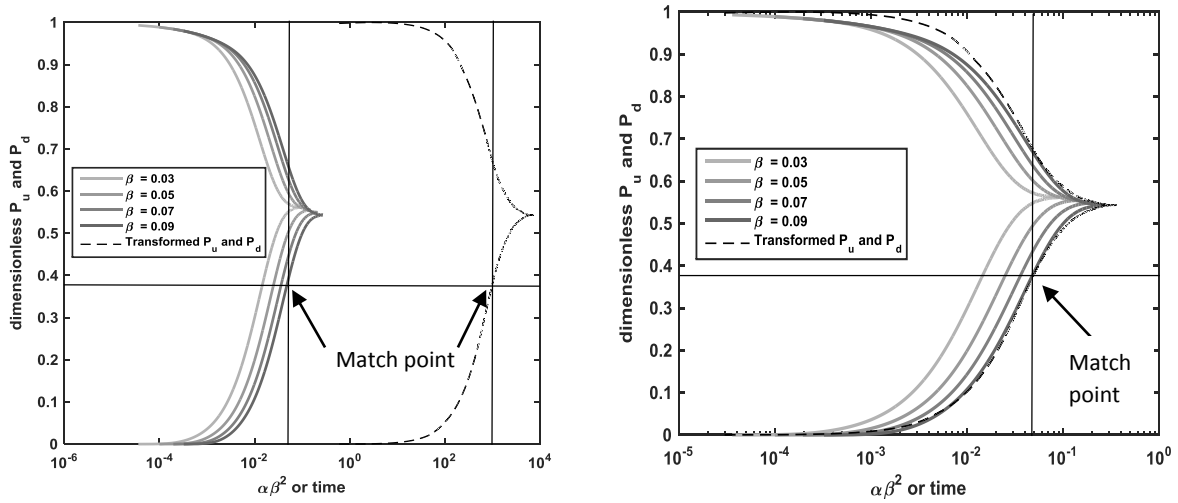

Figure 9: Left figure is before translation and Right one is after translation for matching

Table 1 represents the results from the proposed approach for the five sequences. Every row represents one of the five experiments. The second column shows the equilibration pressure for every pulse decay experiment. The third column shows the exact value of the pulse magnitude; this was ideally intended to be 200 psi exactly, but the deviation is not significant. The fourth, fifth and sixth columns represents the matching parameters for every sequence that were obtained through type curve matching. The seventh and eighth column show the trends of both porosity and permeability calculated using equations (40) and (41).

	Equilibration Pore Pressure, psi	Pulse Size, psi	β	$\alpha\beta^2$	matched time	ϕ(fraction)	k (md)
1st Sequence	246.5	199.5	0.35	0.4	3850	0.076958	1.36E-02
2nd Sequence	362.5	203.5	0.25	0.14	2000	0.067655	2.46E-02
3rd Sequence	470	197.5	0.3	0.175	1650	0.093277	1.92E-02
4th Sequence	580	200	0.23	0.35	1500	0.075657	2.25E-02
5th Sequence	696.5	200	0.09	0.044	1070	0.030271	7.22E-02

Table 1: Results from the proposed method for the five sequences of the pulse decay experiment

In addition, the pressure decay data presented in figure 5 was interpreted using the straight-line method based on the slightly compressible fluid flow model (Jones 1997) for comparison purposes. In the straight-line method, the dimensionless pressure data is plotted as a function of time on a semi-log scale as shown in figure 10. Permeability can be calculated from the slope of the straight-line fit to the data using equations (42) and (43).

$$\Delta P_D = \left(\frac{P_u^2(t) - P_d^2(t)}{P_u^2(1) - P_d^2(1)} \right) \tag{42}$$

$$k_g = -\frac{14696 m_1 (\mu_g c_g) L}{f_1 A \left(\frac{1}{V_1} + \frac{1}{V_2} \right)} \tag{43}$$

It can be seen from Figure 10 that the characteristic slope of each pulse changes from the 1st to the 5th sequence. Pressure decay becomes larger and equilibration is faster for the last pulse, at higher pore pressure and lower net effective stress.

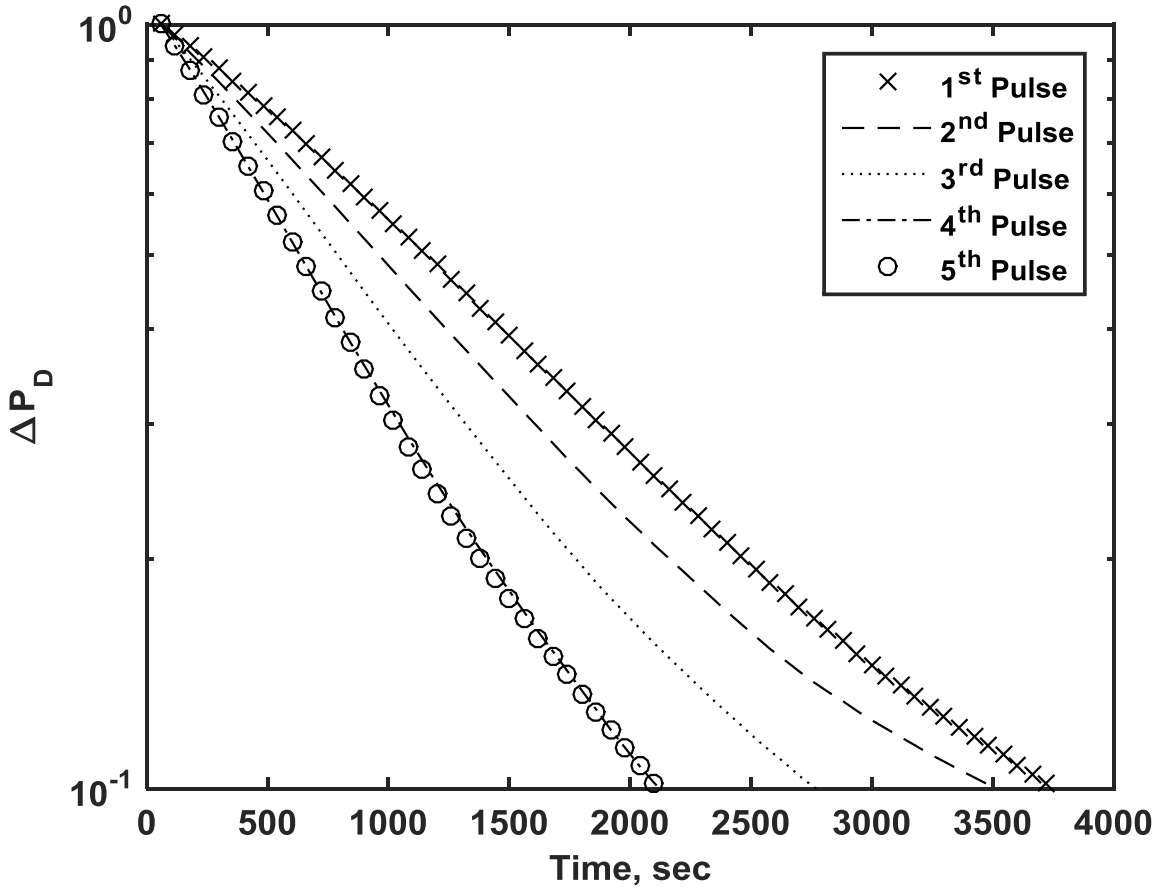

Figure 10: Dimensionless upstream-downstream pressure difference as a function of time for pulse decay experiment in Marcellus shale core

Table (2) shows the summary of the results from the straight-line method. Similar to table (1), each row in table (2) corresponds to one of the five pulse decay sequences. The second column is for the slopes (m_1) of the straight lines graphed in figure (10). The third column is the viscosity of Argon at the equilibration pressure of every experiment and this was obtained from

"NIST Tables of Thermodynamics" ((NIST)). The fourth column is for the compressibility factor of argon at the equilibration pore pressures; further details on how to calculate it is shown in appendix-B. The fifth column is the product of the third and fourth. The last column is for the calculated values of permeability for every experiment; this was calculated using equation (43). It should be noted that column two and five had opposite trends; the absolute value of the latter was increasing and the former was decreasing. The permeability in the last column is made by the product of the columns two, five and other numbers that are constant; therefore, it mainly depends on the values in columns two and five. That's why they were originally placed in table (2) due to their importance. It can be found that the trend of permeability is masked by the trend of the numbers in the fifth column; and thus, it was decreasing as the pore pressure was increasing. The last column is plotted separately as a function of effective stress in figure (11).

	Slopes ($\Delta P_D/time$), sec^{-1}	μ, cp	Compressibility, psi^{-1}	μc	K_g (md)
1st Sequence	2.37E-04	0.022781	0.004000541	9.11E-05	9.91E-03
2nd Sequence	2.51E-04	0.022961	0.002778142	6.38E-05	2.43E-03
3rd Sequence	3.00E-04	0.023154	0.002127929	4.93E-05	1.12E-03
4th Sequence	4.09E-04	0.023358	0.001724348	4.03E-05	7.06E-04
5th Sequence	4.09E-04	0.023594	0.001428738	3.37E-05	7.88E-04

Table 2: Results from a straight-line method

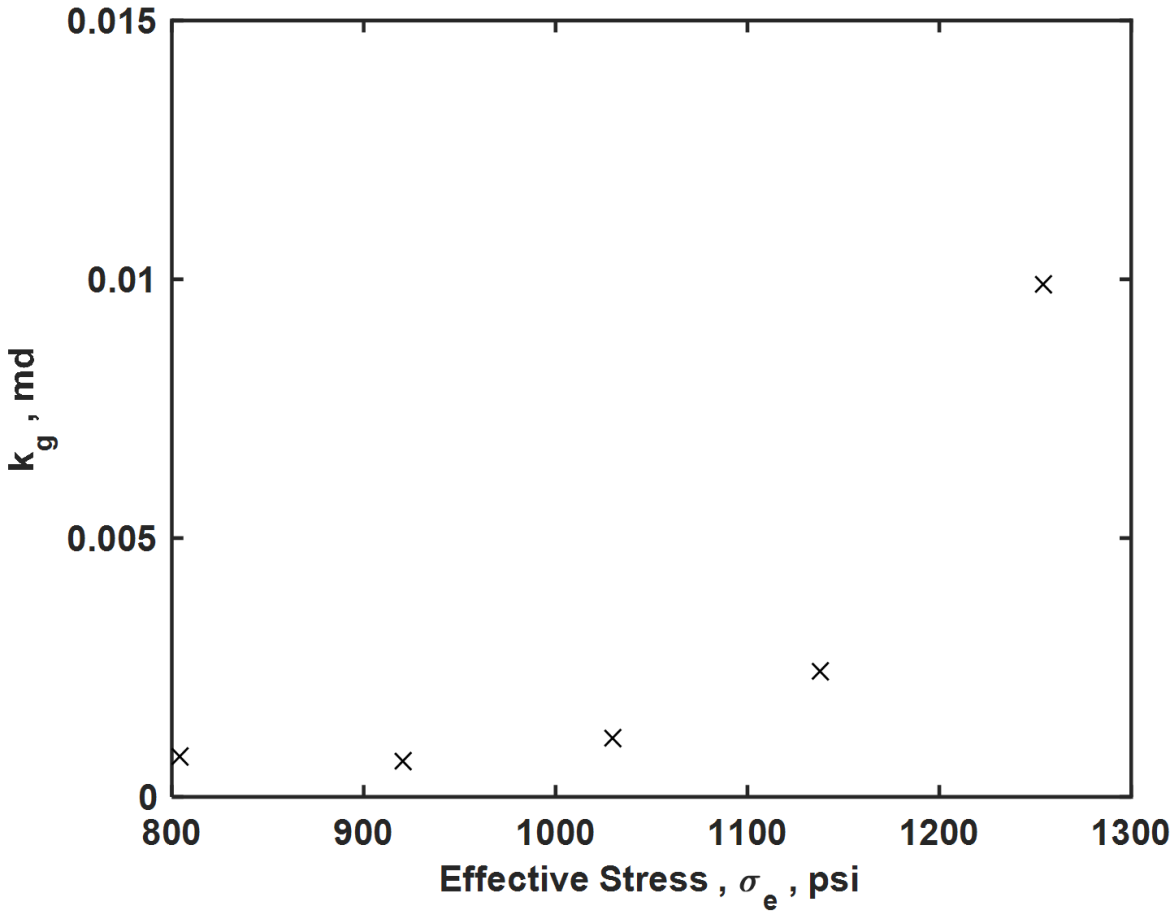

Figure 11: Permeability trends obtained by using a straight-line method

Figure 12 presents a comparison between the straight-line method and the proposed method as they are both plotted against the effective stress. It can be seen that the permeability estimates for the pulse decay sequences in this work using both methods are different in terms of trends and values. Those differences between the two methods are going to be analyzed in the discussion section.

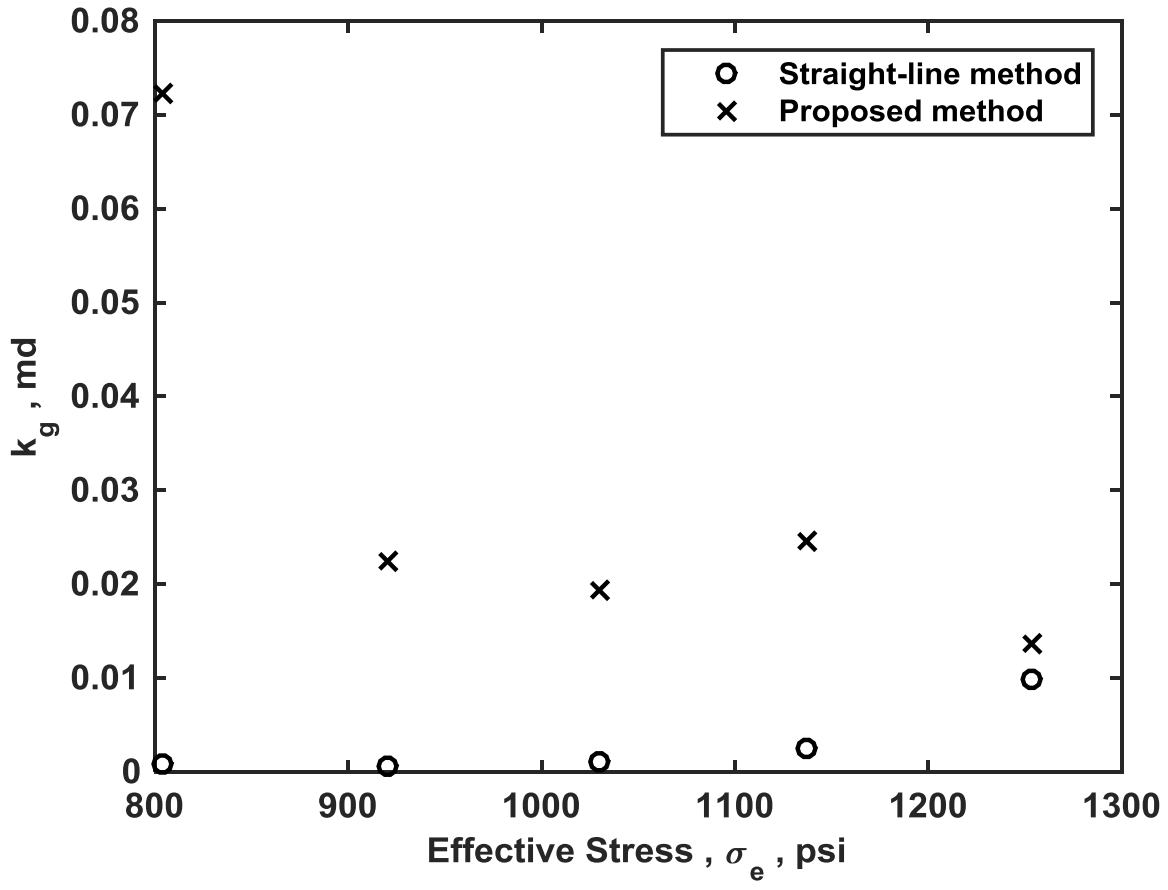

Figure 12: permeability trends obtained using the proposed method in comparison to the straight-line method

Chapter 5. Discussion

The purpose of this research is to add an improvement on the pulse decay analysis technique so that it can better evaluate low initial pressure and high pulse magnitude pulse decay experiments. The method was put into examination by applying it on five pulse decay sequences that were made at relatively low initial pore pressure and high pulse magnitude. In addition, the sequences were analyzed by another method based on the slightly compressible flow model (Jones 1997) which is much simpler to deal with compared to the proposed method.

In terms of results, there are four major key findings that are worth mentioning. First, when the proposed method was used, the permeability was found to be inversely proportional to the effective stress. Second, when the five pulse decay sequences were analyzed with the slightly compressible flow equations (Jones 1997), the permeability was found to be directly proportional to the effective stress. Third key finding is that according to figures 4 a,b and c, the higher the pore pressure the more closer normalized pseudo-pressure and normal pressure curves are. Fourth finding, there was an early time mismatch between experimental data and type curves that was always appearing in all experiments at the upstream curve.

Regarding the first key finding, the trend that was found agrees with literature (Heller *et al.*2014) which suggests that the pseudo pressure approach can detect changes in permeability at low initial pressures and high pulse magnitude. With reference to the second key finding, it can be shown that the changes in viscosity and compressibility are not taken into consideration in the slightly compressible governing equation. Although the rate of pulse decay $\frac{\Delta P_D}{\Delta time}$ (column 2 in table 2) was showing the expected trends, the overall equation or more specifically the

product of viscosity and compressibility distorted this trend. With respect to the third key finding, the similarity of the normalized normal and pseudo pressure curves at high pressures can be explained by figure (13). It can be seen that the product of viscosity and compressibility start to change in a slight manner starting 500- 700 psi. In fact, the curve in figure (13) starts to have an asymptotic behavior above 1000 psi; starting from such pressure, for Argon gas, both methods should give the exact same result. With regards to the fourth key finding, the same observation was made by (Brace, Walsh, and Frangos 1968) and was attributed to thermal effects due to the sudden introduction of a pressure-pulse. Those thermal effects are due to the Joule- Thompson effect due to the sudden increase in pressure in a relatively small volume, which lead to an increase in temperature. This deviation from the theoretical curves are more in the upstream than the downstream as the pulse is introduced from the upstream. However, as time progressed those thermal effects disappeared and thus a good match between the mathematical model and experimental data was found.

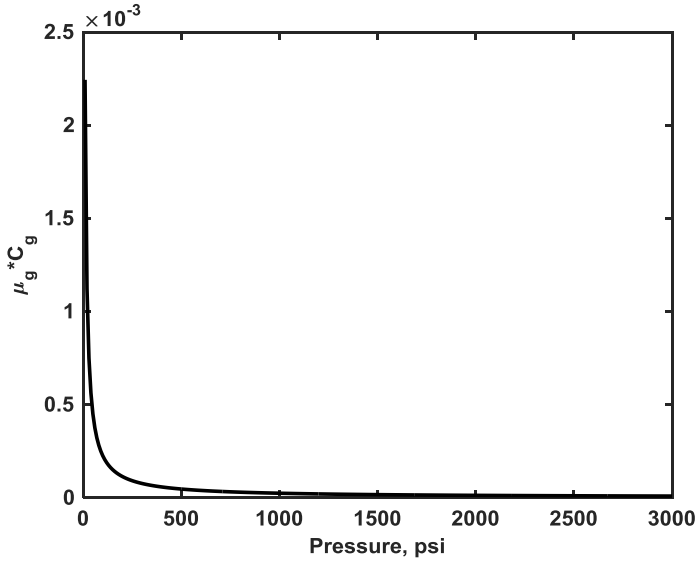

Figure 13: The product of viscosity and compressibility for Argon as a function of Pressure

There are two apparent limitations for this work. First, the mathematical fluid flow model for this work does not account for the "Klinkenberg effect". It is known from (Klinkenberg 1941) that at low pressures, slippage of gas molecules should be expected and that the apparent permeability will be higher than the absolute permeability. Therefore, it should be noted that the permeability that is calculated from this work is the result of two parameters. The first parameter is the change in the effective stress and the second one is the slippage. The proposed method produces the total permeability change in a combined manner rather than getting the separate contribution of changes due to slippage and ones due to changes in effective stress.

Second apparent limitation is that, it can be thought that the method being proposed is rather demanding and one can circumvent all of that by designing the pulse decay experiment at high pore pressure and small pulses. Knowing that the logic behind such design (high pore pressure and small pulses) is to avoid slippage (Klinkenberg 1941) and the fact that gases act as liquids at high pressures and thus the assumption of slightly compressible fluid can work.

The reply for that would be: many of the important shale gas reservoirs in the US reached a low pressure (Shi et al. 2013) during its depletion that is similar to the pore pressures in the experiments in this work. In order to be able to get the permeability of shale gas at these low pore pressures, the pore pressure in the pulse decay experiments should be taken to a relatively low one as the ones used in the experiments in this work. At these low pressures, only the pseudo-pressure approach can analyze the pulse decay experiments.

Chapter 6. Conclusions and Recommendations

In this work, an improved pseudo-pressure type-curve approach has been presented to better estimate the permeability and porosity from pressure-pulse decay data at low pore-pressures and high pulse magnitude. The following conclusions were obtained from the work presented above:

1- The proposed method adds to the literature an improved method to analyze low initial pressure and high pulse magnitude pressure-decay experiments.

2- The oversimplifications incurred in the straight-line method for permeability estimates, which are based on the slightly compressible flow model, result in unrealistic permeability behavior as a function of net stress conditions. This problem was resolved by using the proposed approach.

3- The proposed method is valid within a wide range of β (ratio of compressive storage in pore volume to one in upstream) such that $0.001<\beta<10$. The reason is that graphically the curves tend to be the same below 0.001 and above 10 (Hsieh et al. 1981). This is an advantage over the straight-line method, which requires the ratio between compressive storage of the sample and the compressive storage of both upstream and downstream to be close to 1.0.

4- The pseudo pressure approach and slightly compressible governing equations behave similarly at high pressures and low pulse magnitudes.

Although the results presented in this work shows the dependence of permeability on changes in stress conditions and fluid properties, more work can be done in order to separate the effects of changes in stress conditions and changes in fluid properties on permeability.

		Boundary (vertical and radial) stresses								
		300	500	700	900	1100	1300	1500	1700	1900
Pore Pressure	200	100	300	500	700	900	1100	1300	1500	1700
	400		100	300	500	700	900	1100	1300	1500
	600			100	300	500	700	900	1100	1300
	800				100	300	500	700	900	1100
	1000					100	300	500	700	900

Table 3: Several combinations of boundary stresses and pore pressures and their corresponding values of net stresses

Table 3 shows different combinations of boundary (vertical and radial) stresses and pore pressures and their corresponding value of net stresses. For example: at a boundary stress of value of 300 psi (2nd row and 3rd column) and pore pressure of 200 psi (3rd row and 2nd column), the corresponding net stress is equal to 100 psi. The experiments that were done in this work correspond to the 9th column, where the boundary stresses were set to be constant and the pore pressure was progressively increasing from one pulse to another.

It should be noted that, if the sequences of the pulse decay are made in a horizontal direction with reference to table 3, the pore pressure would be constant and the boundary stresses will be changing. Therefore, the change in permeability, if any, should be attributed only to changes in stress conditions without any slippage. However, if the pulse decay sequences are made diagonally, as marked

in yellow, blue…etc., the changes in permeability are going to be only attributed to the slippage effects (Klinkenberg effect) because, in the diagonal direction, the net stresses were constant and the pore pressure was changing.

In this work, the pulse decay sequences were done in a vertical direction, with reference to table 3, where the changes in permeability were due to changes in net (effective stresses) and pore pressures (slippage effects). It is recommended for future work that more pulse decay experiments should be done in both horizontal and diagonal direction, with reference to table 3, in order to be able to separate the effect of net stresses and slippage on permeability.

References

(NIST), National Institute of Standards and Technology. Web.

Al-Hussainy, R., H. J. Ramey, Jr., and P. B. Crawford. 1966. 'The Flow of Real Gases Through Porous Media', *Journal of Petroleum Technology*.

Boitnott, G. N. 1997. "Use of Complex Pore Pressure Transients to Measure Permeability of Rocks." In *SPE Annual Technical Conference and Exhibition*. Society of Petroleum Engineers.

Bourbie, Thierry, and Joel Walls. 1982. 'Pulse Decay Permeability: Analytical Solution and Experimental Test', *Society of Petroleum Engineers Journal*.

Brace, W. F., J. B. Walsh, and W. T. Frangos. 1968. 'Permeability of Granite under High Pressure', *Journal of Geophysical Research*, 73: 2225-36.

Cui, X., A. M. M. Bustin, and R. M. Bustin. 2009. 'Measurements of gas permeability and diffusivity of tight reservoir rocks: different approaches and their applications', *GEOFLUIDS*, 9: 208-23.

Dicker, A. I., and R. M. Smits. 1988. "A Practical Approach for Determining Permeability From Laboratory Pressure-Pulse Decay Measurements." In *International Meeting on Petroleum Engineering*. Society of Petroleum Engineers.

Fischer, G. J. 1992. 'Fault Mechanics and Transport Properties of Rocks - A Festschrift in Honor of W. F. Brace Chapter 8 The Determination of Permeability and Storage Capacity: Pore Pressure Oscillation Method', *International Geophysics*, 51: 187-211.

Haskett, Steven E., Gene M. Narahara, and Stephen A. Holditch. 1988. 'A Method for Simultaneous Determination of Permeability and Porosity in Low-Permeability Cores', *SPE Formation Evaluation*

Hsieh, P. A., J. V. Tracy, C. E. Neuzil, J. D. Bredehoeft, and S. E. Silliman. 1981. 'A transient laboratory method for determining the hydraulic properties of 'tight' rocks—I. Theory', *International Journal of Rock Mechanics and Mining Sciences and Geomechanics Abstracts*, 18: 245-52.

Jin, Guodong, Héctor Gonzàlez Pérez, Ali Abdullah Al Dhamen, Syed Shujath Ali, Asok Nair, Gaurav Agrawal, Mohamed R. Khodja, Syed Rizwanullah Hussaini, Zaid Zaffar Jangda, and Abdulwahab Zaki Ali. 2015. "Permeability Measurement of Organic-Rich Shale - Comparison of Various Unsteady-State Methods." In *SPE Annual Technical Conference and Exhibition*. Society of Petroleum Engineers.

Jones, S. C. 1997. 'A Technique for Faster Pulse-Decay Permeability Measurements in Tight Rocks', *SPE Formation Evaluation*.

Kamath, J., R. E. Boyer, and F. M. Nakagawa. 1992. 'Characterization of Core Scale Heterogeneities Using Laboratory Pressure Transients', *SPE Formation Evaluation*.

Klinkenberg, L. 1941. "The Permeability Of Porous Media To Liquids And Gases." In *API 11th mid year meeting*. Tulsa.

Neuzil, C. E., C. Cooley, S. E. Silliman, J. D. Bredehoeft, and P. A. Hsieh. 1981. 'A transient laboratory method for determining the hydraulic properties of 'tight' rocks—II. Application', *International Journal of Rock Mechanics and Mining Sciences and Geomechanics Abstracts*, 18: 253-58.

Shi, Juntai, Lei Zhang, Yuansheng Li, Wei Yu, Xiangnan He, Ning Liu, Xiangfang Li, and Tao Wang. 2013. "Diffusion and Flow Mechanisms of Shale Gas through Matrix Pores and Gas Production Forecasting." In *SPE Unconventional Resources Conference Canada*. Society of Petroleum Engineers.

Zamirian, Mehrdad, Kashy Kashy Aminian, Samuel Ameri, and Ebrahim Fathi. 2014. "New Steady-State Technique for Measuring Shale Core Plug Permeability." In *SPE/CSUR Unconventional*. Resources Conference – Canada: Society of Petroleum Engineers.

Appendix A- Sample calculation of ϕ_m Roots

The solution for ϕ_m's (roots of the equation) in this work is going to be obtained numerically using Newton-Raphson technique as following:

$$F = tan\phi_m - \frac{(1+\gamma)\phi_m}{\frac{\gamma\phi_m^2}{\beta} - \beta}$$

$$F' = Sec^2\phi_m - \frac{\left((1+\gamma)\left(\frac{\gamma\phi_m^2}{\beta} - \beta\right) - \left(\frac{2\gamma\phi_m}{\beta}\right)\left((1+\gamma)\phi_m\right)\right)}{\left(\frac{\gamma\phi_m^2}{\beta} - \beta\right)^2}$$

$$\phi_{m,new} = \phi_{m,old} - \frac{F}{F'}$$

It should be noted that equation (37) has infinite roots. However, one only needs the first two or three positive roots for the solution to work. In order for the numerical scheme to start, one has to make an initial guess for the ϕ_m and keep iterating till the $error = abs(\phi_{m,new} - \phi_{m,old})$ becomes very small (ex: 0.0001).

for $\gamma = 1$ and $\beta = 0.001 \rightarrow$ 1:

	Initial Guesses	ϕ_1	ϕ_2	ϕ_3
β = 0.001	0→ 5	0.044718		
β = 0.003	0→ 5	0.07744		
β = 0.01	0→ 5	0.141304		

β = 0.03	0→ 5	0.244338		
β = 0.1	0→ 5	0.443521	3.203994	
β = 0.3	0→ 5	0.755755	3.321733	
β = 1	1.5→5	1.306542	3.673194	6.58462

Appendix B- Procedure of the Pseudo Pressure transformation

In order to convert the upstream and downstream data to pseudo-pressures, a numerical integration technique may be used like trapezoidal rule to produce a table for pressure values that corresponds to pseudo-pressure values. A simple computer code can then manifest linear interpolation and convert all the upstream and downstream pressures to pseudo-pressures.

An example for the numerical integration of equation (2) for two pressure points is shown in following two equations.

$$P_{p_1} = 2\left[\frac{1}{2} * \left(\frac{P_1}{\mu_1 z_1}\right) * P_1\right]$$

$$P_{p_2} = 2.\left[\frac{1}{2} * \left(\frac{P_1}{\mu_1 z_1}\right) * P_1 + \frac{1}{2}\left(\frac{P_1}{\mu_1 z_1} + \frac{P_2}{\mu_2 z_2}\right) * (P_2 - P_1)\right]$$

If the trapezoidal rule is applied on the entire pressure range of interest for Argon (gas used in the experiments), figure (14) should be the result.

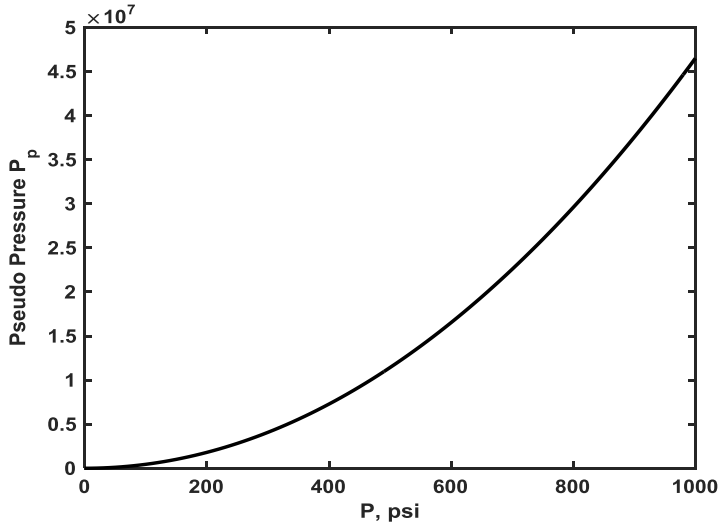

Figure 14: Pseudo-pressure transformation Chart

The calculation of fluid properties c_g , Z , and μ required for the pseudo-pressure transformation is presented next.

PENG-Robinson EOS is used to obtain the compressibility factor Z :

$$\alpha = \left[1 + (0.37464 + 1.54226\omega - 0.26992\omega^2)\left(1 - \sqrt{T_r}\right)\right]^2$$

$$a = 0.45724\frac{R^2T_c^2}{P_c}$$

$$b = 0.07780\frac{RT_c}{P_c}$$

$$A = \frac{\alpha aP}{R^2T^2}$$

$$B = \frac{bP}{RT}$$

$$Z^3 - (1-B)Z^2 + (A - 2B - 3B^2)Z - (AB - B^2 - B^3) = 0$$

To obtain gas compressibilityC_g:

$$c_g = \frac{1}{P}\left[1 - \frac{dln(z)}{dln(p)}\right]$$

In order to get it for every pressure point:

$$c_{g,i} = \frac{1}{P_i}\left[1 - \frac{(\ln(z_{i-1}) - \ln(z_{i+1}))}{\ln(p_{i-1}) - \ln(p_{i+1})}\right]$$

The viscosity in this work was obtained from NIST tables for thermodynamics at Temperature = 23 $^\circ$ C